Location of active sites of NiFe hydrogenase determined by the combination of multiple isomorphous replacement and multiwavelength anomalous-diffraction methods.

By YOSHIKI HIGUCHI, TAKUYA OKAMOTO, KIYOSHI FUJIMOTO and SHINTARO MISAKI, *Department of Life Sciences, Himeji Institute of Technology, 1479-1 Kanaji, Kamigori, Ako-gun, Hyogo* 678-12, *Japan*, YUKIO MORIMOTO, *Department of Biological Science and Technology, The University of Tokushima, 2-1 Minamijosanjima, Tokushima* 770, *Japan*, and NORITAKE YASUOKA, *Department of Life Sciences, Himeji Institute of Technology,* 1479-1 *Kanaji, Kamigori, Ako-gun, Hyogo* 678-12, *Japan*

Abstract

The active centers of NiFe hydrogenase from *Desulfovibrio vulgaris* Miyazaki F have been located in the electron-density map calculated at 4 Å resolution. The electron-density map based on five heavy-atom derivatives showed four strong peaks which were clearly distinguished from the protein region. These strong densities have been successfully assigned to three iron–sulfur clusters and one Ni atom by a difference Fourier technique with coefficients of the best phases from the multiple isomorphous replacement (MIR) method and structure factors obtained at five wavelengths (1.040, 1.487, 1.730, 1.743 and 1.750 Å) with the use of a synchrotron radiation source. Four active centers are approximately lined up at a distance of *ca* 13 Å, which seems reasonable if they are connected with the electron-transfer chain.

Introduction

Hydrogenase from the sulfate-reducing bacterium, *Desulfovibrio vulgaris* Miyazaki F, is a membrane protein with two non-equivalent subunits of 62.5 and 28.8 kDa. Its amino-acid sequence was recently determined from the gene sequence (Deckers, Wilson & Voordouw, 1990). Three types of hydrogenases have been found from the genus *Desulfovibrio* in sulfate-reducing bacteria (Prickril *et al.*, 1987), and they are classified as Fe, NiFe and NiFeSe hydrogenases. The hydrogenase in this study is grouped into the NiFe hydrogenases and, from the amino-acid sequence, it is considered to contain two Fe_4S_4 clusters, one Fe_3S_4 cluster and one Ni atom as prosthetic groups (Deckers, Wilson & Voordouw, 1990; Furuichi, Ozaki, Niki & Akutsu, 1990). The presence and the content of Ni and Fe atoms in the hydrogenase from Miyazaki was confirmed by the *K*-edge jump of extended X-ray absorption fine-structure spectroscopy (EXAFS) data (Yasuoka *et al.*, 1993). This protein can catalyze the consumption and the production of molecular hydrogen, and the reactions are coupled with a series of various oxidation–reduction reactions which are associated with an electron-transport chain from sulfate to sulfide. So far two kinds of NiFe hydrogenases have been crystallized and reported from *D. vulgaris* Miyazaki F (Higuchi *et al.*, 1987) and *gigas* (Niviere, Hatchikian, Cambilleau, & Frey, 1987). The structure analysis of the hydrogenase is expected to elucidate the mechanism of hydrogen metabolism and electron transfer between the proteins on a structural basis.

It is well known that the real and imaginary components ($\Delta f'$ and $\Delta f''$) of the scattered X-rays change dramatically when the energy of the incident X-ray beam is across the absorption edge of an element. Owing to the recent excellent tunability of the required X-ray energy and improvement of the technique to maintain stability of synchrotron radiation, the multiwavelength anomalous-diffraction (MAD) method has contributed to the crystal structure analysis of relatively small proteins such as cytochrome *c*-553 (Nakagawa, Higuchi, Yasuoka, Katsube & Yagi, 1990), azurin (Korszun, 1987), ferredoxin (Murthy, Hendrickson, Orme-Johnson, Merritt & Phizackerley, 1988), blue-copper protein (Guss *et al.*, 1988). Hydrogenase from the strain Miyazaki F is also a good candidate for solving the phase problem by using MAD data, because it contains 11 Fe atoms and one Ni atom. We have tried to estimate the phase angles by the multiple isomorphous replacement (MIR) method, and have succeeded in obtaining the initial phases at 4 Å resolution. The electron-density map shows four strong areas of density which could be assigned as the peaks of three iron–sulfur clusters and one Ni atom. Here we report the use of the MAD data to distinguish the peaks of two kinds of anomalous scatterers in the electron-density map. The success of this method suggests that the small changes in anomalous diffraction were effectively observed and the possibility of using the MAD method as a phasing tool for molecules of larger molecular weight.

Crystallization and data collection

Hydrogenase was extracted from the membrane fraction of *D. vulgaris* Miyazaki by a trypsin digestion incubated for 12 h at 277 K. The protein was purified by the method described previously (Yagi *et al.*, 1976; Higuchi *et al.*, 1987). The hydrogenase crystals were originally obtained from a polyethylene glycol solution, but these were not suitable for preparation of heavy-atom derivatives. Therefore, in this study crystals obtained by the vapor-diffusion method, from 50% 2-methyl-2,4-pentanediol, 25 mM Tris–HCl buffer solution (pH = 7.4) in the presence of 0.05% sodium azide at a final protein concentration of 50 mg ml^{-1}, were used for MIR experiments, whereas those from the polyethylene glycol solution were used for the MAD experiment. The introduction of micro seeds into the crystallization droplets was essential to produce large crystals of good quality (Higuchi *et al.*, 1987). The crystals (> 1.0 mm) were grown for several days at 288 K and belonged to space group $P2_12_12_1$ with one molecule per asymmetric unit. Unit-cell dimensions are slightly different from crystal to crystal even in the same crystallization droplets. Therefore, crystals with similar cell dimensions for both native and derivatives were chosen for structure analysis. Typical cell dimensions are $a = 99.73$, $b = 127.93$, $c = 66.68$ Å. Heavy-atom derivatives were prepared by a conventional soaking method using various heavy-atom reagents. In total nine heavy-atom derivatives have been

Table 1. *Summary of heavy-atom refinement at 4 Å resolution*

Space group $P2_12_12_1$, $a = 99.17$, $b = 127.93$, $c = 66.68$ Å, $V = 8.460 \times 10^5$ Å^3.

Derivatives*	Reflections (phased)	Completeness (%)	R_{sym} (%)	K_{over}†	B_{over}‡ (Å^2)	R_{Cullis}§ (Reflections)	No. of sites	Phasing power	Mean figure of merit
NATIVE	7281	96.0	4.46	—	—	—	—	—	0.76
EMTS	7072	93.3	5.28	0.992	−0.658	0.604 (1046)	1	2.26	—
KUOF	7184	94.8	6.37	0.976	0.444	0.757 (1100)	8	1.72	—
K3IR	6925	91.3	4.70	0.993	0.131	0.768 (979)	3	1.20	—
KPTC	6815	89.9	3.34	0.996	0.353	0.978 (977)	1	0.31	—
UOAC	6377	84.1	6.23	0.988	−0.417	0.957 (837)	5	0.91	—

* Derivatives are abbreviated as EMTS, ethyl mercury thiosalicylate; KUOF, $K_3UO_2F_5$; K3IR, K_3IrCl_6; KPTC, K_2PtCl_6; UOAC, uranyl acetate.
† Overall scale factor for each derivative to native crystal.
‡ Overall relative temperature factor for each derivative to native crystal.
§ $R_{Cullis} = \Sigma||F_{PH}(obs) \pm F_P(obs)| - F_H(calc)|/\Sigma|F_{PH}(obs) - F_P(obs)|$ for all centric reflections.

Table 2. *Expected values of real and imaginary components of anomalous scattering from* Fe *and* Ni *atoms at given X-ray wavelengths and some statistical values of MAD data at 4 Å resolution*

Data set (Å)	Fe*		Ni*		Anomalous difference ratio† (%)					R_{sym}	R_{merge}§	Reflections	Completeness
	$\Delta f'$	$\Delta f''$	$\Delta f'$	$\Delta f''$	1.040 Å	1.743 Å	1.730 Å	1.750 Å	1.487 Å				
1.040	0.20	1.66	−0.05	2.16	3.90	7.85	6.82	7.31	5.09	4.25	6.19	6716	88.6
1.743	−9.21	‡	−1.75	0.63	—	4.58	5.17	5.96	6.82	5.73	7.08	5139	67.8
1.730	−4.49	3.89	−1.78	0.63	—	—	6.52	5.17	5.87	6.88	7.74	5165	68.1
1.750	−5.33	0.47	−1.72	0.64	—	—	—	4.39	6.40	5.35	6.60	5095	67.2
1.487	−0.79	2.97	−7.39	‡	—	—	—	—	5.29	5.54	6.26	5779	76.2

* The values are not experimentally evaluated from methods such as EXAFS, but quoted from the table in Sasaki (1989), *Numerical Tables of Anomalous Scattering Factors Calculated by Cromer and Liberman's Method*, pp. 16–17, 53–54.
† Dispersive difference ratios are given in off-diagonals, whereas Bijvoet difference ratios are in diagonal elements.
‡ The $\Delta f''$ values at these wavelengths cannot be estimated from the theoretical curve because of the abrupt change of the values of $\Delta f''$ the imaginary part in the region near the absorption edge of the anomalous scatterers. These depend on the degree of the accuracy of the X-ray wavelengths.
§ R_{merge} values were calculated for all measured full reflections obtained with the use of a Weissenberg camera at the Photon Factory.

prepared, and they show distinctive intensity changes from the native crystals. They are ethyl mercury thiosalicylate (EMTS), $K_3UO_2F_5$ (KUOF), K_3IrCl_6 (K3IR), K_2PtCl_6 (KPTC), sodium mersalate (MERS), phenylmercury acetate (PHHG), uranyl acetate (UOAC), europium chloride (EUCL), and trimethyllead acetate (TMLA) derivatives. Diffraction images for MIR and MAD experiments were recorded using a Weissenberg camera for macromolecular crystallography with a Fuji imaging plate at station BL-6A2 of the Photon Factory, National Laboratory for High Energy Physics, Tsukuba, Japan (Sakabe, 1991). The beam path from the source to the detector was filled with helium gas. The wavelength of X-rays used for the MIR method was 1.040 Å, whereas five wavelengths were chosen for the MAD experiment. The energy at the absorption edges of Fe (1.743 Å), Ni (1.487 Å) and Au (1.040 Å) atoms was calibrated at the mid point between the first inflection and the maximum absorption point through iron, nickel and gold foils inserted between two ion chambers in the upper and lower stream of X-rays. The wavelengths near the K absorption edge of the Fe atom (1.730, 1.750 Å) were tuned by the angular settings of the silicon (111) monochromator. For the MAD experiment, diffraction data sets from each X-ray wavelength were collected at different positions in the same crystal by moving the crystal along the spindle axis of the camera in order to reduce radiation damage. In addition, the data are expected to

be free from the scaling errors and lack of isomorphism among the data sets because the diffraction patterns were measured from the same crystal. The diffraction images were indexed by the program *UWEIS*, which is a modified version of the original program *WEIS* (Higashi, 1989), and *XVIEWER* (Fujii, Morimoto, Nakagawa, Higuchi & Yasuoka, 1994), and scaled to final data sets using absorption-corrected structure factors (6 Å) collected by a four-circle diffractometer as reference data.

MIR phasing

The heavy-atom parameters of the six derivatives found initially (EMTS, KUOF, K3IR, KPTC, MERS, PHHG) were refined by *PHARE* (Blow & Matthews, 1973; Bricogne, 1982) from the *CCP4* package (SERC Daresbury Laboratory, 1979). The correct enantiomorph was chosen from the mean figure of merit which was calculated with the anomalous-dispersion effect of heavy-atom derivatives. In the initial electron-density map at 4.0 Å calculated with best phases, there were large negative peaks at the position of heavy-atom sites with high occupancies, and also consecutive ghost peaks around these negative peaks. These abnormal features around heavy-atom sites were considered to be caused by the lack of the isomorphism of derivative crystals. They made interpretation
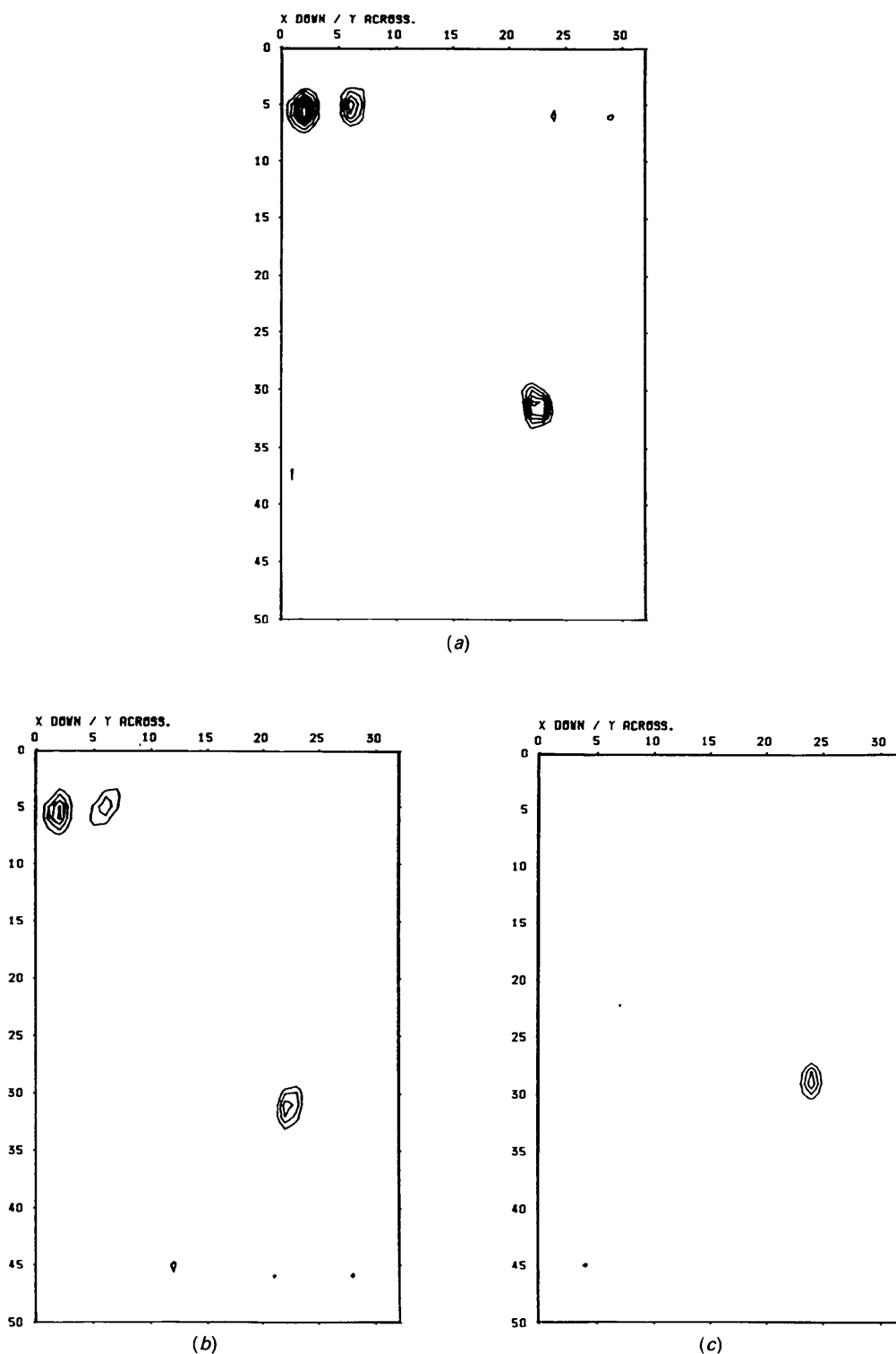
Fig. 1. Anomalous-difference maps calculated with phases obtained from final MIR data at 4 Å resolution. For each map an asymmetric unit of the crystal is presented. Representative z sections of (a) a dispersive difference electron-density map (z = 2/32 − 5/32) for Fe atoms calculated with coefficients of $|F_{1.040\,Å} - F_{1.743\,Å}| \exp(i\alpha_{best})$; ($b$) a Bijvoet difference map (z = 2/32 − 5/32) for Fe atoms with $|F_{1.730\,Å}(+) - F_{1.730\,Å}(-)| \exp(i\alpha_{best} - \pi/2)$; and ($c$) a dispersive-difference map (z = 9/32) for an Ni atom with $|F_{1.04\,Å} - F_{1.487\,Å}| \exp(i\alpha_{best})$ are presented. The maps are contoured in intervals of 2σ starting at 3σ above the mean density level. The strong densities which could be assigned to three iron clusters [(a) and (b)] and one Ni atom (c) can be seen in the maps.

of the MIR map difficult within 15 Å of the heavy-atom sites. The abnormal features were reduced by applying local scaling (Matthews & Czerwinski, 1975) to the structure factors of nine derivatives (the six derivatives found initially and described above, and the three derivatives of UOAC, EUCL, TMLA). The local scaling factors were calculated from the equation $\sum F_{PH}^2 / \sum F_P^2$ in local areas which contain 50 reflections, where F_P are structure factors of the native crystal and F_{PH} are those of derivative crystals. Four out of nine derivatives were excluded from MIR phasing because of a lack of isomorphism. Heavy-atom parameters were re-refined by *PHARE* at 4.0 Å resolution. In this case anomalous-dispersion effects of derivatives were not included, because they did not improve the statistical values such as figures of merit and the phasing power of derivative crystals. A summary of data-collection and phasing statistics for the derivatives is shown in Table 1. A new electron-density map at 4.0 Å resolution was calculated with the new figures of merit and the best phases. The negative and ghost peaks around the heavy-atom sites disappeared in the new map. There were four strong features in this map, and they were easily distinguished from the electron density of the apo-protein region.

Location of active centers

Three iron–sulfur clusters and one Ni atom were unambiguously located in the difference map based on the structure-factor data obtained from multiwavelength X-ray diffraction. Five X-ray wavelengths, 1.040, 1.487, 1.730, 1.743 and 1.750 Å, were chosen for this purpose. The expected $\Delta f'$ and $\Delta f''$ values of the Fe and Ni atoms for each wavelength are shown in Table 2. Though they were not quantitatively estimated by the EXAFS experiment but quoted from the table calculated by Sasaki (1989), dispersive and Bijvoet anomalous differences were possibly detected in the hydrogenase diffraction pattern. Statistical values of the MAD data are shown in Table 2. Anomalous-dispersion effects were effectively observed according to the dispersive difference ratios between data sets and the Bijvoet difference ratio of data at 1.730 Å.

To distinguish iron–sulfur clusters from an Ni atom, various dispersive difference Fourier maps were calculated and examined. In the difference Fourier map with coefficients of $|F_{1.040\,Å} - F_{1.730\,Å}|\exp(i\alpha_{best})$ (not shown), $|F_{1.040\,Å} - F_{1.743\,Å}|$ $\exp(i\alpha_{best})$ (Fig. 1a), and $|F_{1.040\,Å} - F_{1.750\,Å}|\exp(i\alpha_{best})$ (not shown), three distinctive peaks were present in all difference maps, and their positions were consistent with the three out of four strong features in the electron-density map of hydrogenase at 4.0 Å resolution. Furthermore, they were also interpreted in the Bijvoet difference map from the 1.730 Å data (Fig. 1b) using the best phases retarded by $\pi/2$. These peaks could be deduced as iron–sulfur clusters because the magnitude of the coefficients of the dispersive and Bijvoet difference maps were mainly contributed to by the $\Delta f'$ and $\Delta f''$ values of the Fe atoms. The remaining peak was assigned to the Ni atom from the dispersive difference Fourier map with the coefficients based on the $\Delta f'$ value of an Ni atom, that is $|F_{1.040\,Å} - F_{1.487\,Å}|\exp(i\alpha_{best})$ (Fig. 1c). The distances between the three clusters and the Ni atom in the unit cell are shown in Table 3. The Ni atom is located near one cluster (cluster A in Table 3). This cluster is related to cluster B by a distance of 13.1 Å, and cluster B is located at a distance of 12.2 Å from cluster C. Each electron-transfer center was related one dimensionally within a distance of 14 Å (Ni–cluster A–cluster B–cluster C). The distance seems to be reasonable for the clusters to be

Table 3. *Distances between three iron–sulfur clusters and one* Ni *atom assigned in the same molecule*

	Coordinates			Distances (Å)		
	$x/99.17$	$y/127.93$	$z/66.68$	Cluster B	Cluster C	Ni
Cluster A	0.63	0.35	0.12	13.1	24.3	13.8
Cluster B	0.59	0.40	0.96	—	12.2	22.4
Cluster C	0.61	0.47	0.84	—	—	32.5
Ni	0.56	0.38	0.29	—	—	—

connected with electron transfer between them. The hydrogen-processing and electron-conducting functions are considered to be separate in this enzyme. Voordouw (1992) suggested that the hydrogen-processing subunit was an α-subunit with one nickel and one iron–sulfur cluster (Ni–H cluster), whereas the electron-conducting subunit was a β-subunit containing two iron–sulfur clusters, by considering the invariant residues in the 16 sequences of hydrogenases available. According to the relative disposition, the Ni–H cluster might be Ni and cluster A, but final assignment should be postponed until interpretation of the electron-density map of hydrogenase is completed.

MIR phasing has now been extended to 2.8 Å resolution, and model building based on the solvent-flattened map (Wang, 1987) is in progress. Interpretation of the positions of the clusters by the procedure mentioned above is very helpful for chain tracing because iron–sulfur clusters are held by S atoms of cysteine residues.

References

BLOW, D. M. & MATTHEWS, B. W. (1973). *Acta Cryst.* A29, 56–62.
BRICOGNE, G. (1982). *Computational Methods in Crystallography*, edited by D. SAYRE, pp. 223–230. Oxford: Clarendon Press.
DECKERS, H. M., WILSON, F. R. & VOORDOUW, G. (1990). *J Gen. Microbiol.* 136, 2021–2028.
FUJII, I., MORIMOTO, Y., NAKAGAWA, A., HIGUCHI, Y. & YASUOKA, N. (1994). *Bioimages*, 2, 47–52.
FURUICHI, H., OZAKI, Y., NIKI, K. & AKUTSU, H. (1990). *J. Biochem.* 108, 707–710.
GUSS, J. M., MERRITT, E. A., PHIZACKERLEY, R. P., HEDMAN, B., MURATA, M., HODGSON, K. O. & FREEMAN, H. C. (1988). *Science*, 241, 806–811.
HIGASHI, T. (1989). *J. Appl. Cryst.* 18, 129–130.
HIGUCHI, Y., YASUOKA, N., KAKUDO, M., KATSUBE, Y., YAGI, T. & INOKUCHI, H. (1987). *J. Biol. Chem.* 262, 2823–2825.
KORSZUN, Z. R. (1987). *J. Mol. Biol.* 196, 413–419.
MATTHEWS, B. W. & CZERWINSKI, E. W. (1975). *Acta Cryst.* A31, 480–487.
MURTHY, H. M. K., HENDRICKSON, W. A., ORME-JOHNSON, W. H., MERRITT, E. A. & PHIZACKERLEY, P. (1988). *J. Biol. Chem.* 263, 18430–18436.
NAKAGAWA, A., HIGUCHI, Y., YASUOKA, N., KATSUBE, Y. & YAGI, T. (1990). *J. Biochem.* 108, 701–703.

NIVIERE, V., HATCHIKIAN, C., CAMBILLEAU, C. & FREY, M. (1987). *J. Mol. Biol.* **195**, 969–971.

PRICKRIL, B. C., HE, S.-H., LI, C., MENON, N., CHOI, E.-S., PRZYBYLA, A. E., DERVARTANIAN, D. V., PECK, H. D. JR, FAUQUE, G., LEGALL, J., TEIXEIRA, M., MOURA, I., MOURA, J. J. G., PATIL, D. & HUYNH, B. H. (1987). *Biochim. Biophys. Res. Commun.* **149**, 369–377.

SAKABE, N. (1991). *Nucl. Instrum. Methods,* **303**, 448–463.

SASAKI, S. (1989). *Numerical Tables of Anomlous Scattering Factors Calculated by Cromer and Liberman's Method,* pp. 16–17, 53–54. National Laboratory for High Energy Physics, KEK, Tsukuba, Japan.

SERC Daresbury Laboratory (1979). *CCP4. A Suite of Programs for Protein Crystallography.* SERC Daresbury Laboratory, Warrington WA4 4AD, England.

VOORDOUW, G. (1992). *Adv. Inorg. Chem.* **38**, 397–422.

WANG, B. C. (1987). *Methods Enzymol.* **115**, 90–112.

YAGI, T., KIMURA, K., DAIDOJI, H., SAKAI, F., TAMURA, S. & INOKUCHI, H. (1976). *J. Biochem.* **79**, 661–671.

YASUOKA, N., SUGIYAMA, S., MORIMOTO, Y., HIGUCHI, Y., EMURA, S., MAEDA, H., KOTO, K., NAKAI, I. & YOSHIASA, A. (1993). *Jpn. J. Appl. Phys.* **32**, 553–555.